

# ChipletPart: Scalable Cost-Aware Partitioning for 2.5D Systems

Alexander Graening, *Student Member, IEEE*, Puneet Gupta, *Fellow, IEEE*,  
 Andrew B. Kahng, *Fellow, IEEE*, Bodhisatta Pramanik, *Student Member, IEEE*  
 and Zhiang Wang, *Member, IEEE*

**Abstract**—Industry adoption of chiplets has been increasing as a cost-effective option for making larger high-performance systems. Consequently, partitioning large systems into chiplets is increasingly important. In this work, we introduce *ChipletPart*—a cost-driven 2.5D system partitioner that addresses the unique constraints of chiplet systems, including complex objective functions, limited reach of inter-chiplet I/O transceivers, and the assignment of heterogeneous manufacturing technologies to different chiplets. *ChipletPart* integrates a sophisticated chiplet cost model with its underlying genetic algorithm-based technology assignment and partitioning methodology, along with a simulated annealing-based chiplet floorplanner. Our results show that: (i) *ChipletPart* reduces chiplet cost by up to 58% (20% geometric mean) compared to state-of-the-art min-cut partitioners, which often yield floorplan-infeasible solutions; (ii) *ChipletPart* generates partitions with up to 47% (6% geometric mean) lower cost as compared to the prior work *Floorplet*; and (iii) for the testcases we study, heterogeneous integration reduces cost by up to 43% (15% geometric mean) compared to homogeneous implementations. We also present case studies that show how changes in packaging or inter-chiplet signaling technologies can affect partitioning solutions. Finally, we make *ChipletPart*, the underlying chiplet cost model, and a chiplet testcase generator available as open-source tools for the community.

## I. INTRODUCTION

The integration of multiple chips on an interposer has become a favorable approach to reduce the cost of building large systems [1] [2]. In a 2.5D system, a design is decomposed into multiple smaller chiplets, which are packaged together on the same substrate. This splitting can have significant benefits for yield and can enable designs using heterogeneous process technology nodes, going beyond what is possible in a monolithic design. On the other hand, inter-die communication exhibits higher area and power overhead compared to intra-die communication. Due to this and other factors, the potential cost benefits of disaggregation are not always realized [3]. Therefore, it is important to intelligently partition a design into constituent chiplets *and* assign a manufacturing technology to each of the chiplets so as to optimize manufacturing costs.

The natural partitioning granularity for 2.5D integration is at the block-level. Splitting individual IP blocks into multiple chiplets is problematic for design and test methodology reasons as well as for IP reuse. Additionally,

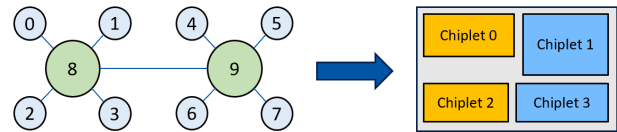


Fig. 1: Generic example of block-level chiplet partitioning. Left: an IP block-level netlist (different types of IP blocks shown in different colors). Right: an integrated 2.5D chiplet system reflecting netlist partitioning with technology node assignment shown by different colors.

splitting an IP block will often have a significant impact on performance and IO count. Due to these considerations, block-level chiplet partitioning (Figure 1) is the focus of this paper. The cost-aware partitioning problem for chiplet systems is fundamentally different from the well-studied [4] [5] [6] netlist min-cut partitioning. The problem size is smaller (usually a few hundred blocks and a few tens of chiplets at most) and the underlying objective function can be complex. Furthermore, inter-chiplet IO reach limitations can render some partitions infeasible, necessitating floorplan-awareness in the partitioner. This is further complicated by the need to select a manufacturing technology for each of the chiplets.

We propose *ChipletPart*, the first open-source, unified framework for chiplet partitioning that combines *cost-driven* multi-way partitioning, heterogeneous technology assignment and IO *reach-aware* floorplanning in a single, automated flow. *ChipletPart* presents a novel adaptation of classical optimizers such as genetic algorithms and simulated annealing to generate floorplan-feasible, cost-optimized and technology-assigned 2.5D chiplet systems. *ChipletPart* is intended for design space exploration before physical implementation.<sup>1</sup> Our key contributions include:

- **Integrated chiplet partitioning with floorplan feasibility:** We present the first unified framework that optimizes system partitioning while guaranteeing feasibility

<sup>1</sup>*ChipletPart* considers a given architecture and generates partitioned chiplets before physical implementation. We do not perform architecture exploration in this work. We envision *ChipletPart* as a tool to assist human designers by generating strong initial solutions, which can then be refined using domain expertise.

under IO reach constraints. In contrast to standard min-cut partitioners (e.g., *hMETIS* [4], *TritonPart* [6]) that ignore floorplan feasibility, *ChipletPart* employs a reach-aware, annealing-based placement engine to guarantee floorplan-legal solutions (Section V-B).

- **Heterogeneous technology assignment:** We handle technology node assignment during partitioning using a genetic algorithm (GA). This enables exploration of cost trade-offs in heterogeneous 2.5D systems—a capability not supported by existing tools such as *FloorPlet* [7] or *Chipletizer* [8]. Our heterogeneous technology-aware, cost-driven, multi-way partitioner, *ChipletPart*, finds cost reductions of up to 43% (6% geometric mean) in multi-technology scenarios. To the best of our knowledge, we are the first work that does technology assignment during partitioning (Section III).
- **Improvements over SOTA:** *ChipletPart* achieves up to 46% improvement in cost over state-of-the-art min-cut based partitioners (*hMETIS* [4], *TritonPart* [6]) that do not guarantee floorplan feasibility. Compared to the *parChiplet* partitioner from *Floorplet* [7], *ChipletPart* generates chiplet solutions that are up to 47% (6% geometric mean) better in cost. Compared to manual partitions, *ChipletPart* generates 24% (7% geometric mean) better solutions (Section VI). Additionally, we explore how variations in technology parameters affect chiplet partitioning (Section VII).
- **Standardized open-source ecosystem:** We translate the Python-based cost model [9] [10] to an equivalent C++ implementation (Section IV-A). This yields a  $5\times$  speedup in cost model execution runtime, and a speedup of more than  $100\times$  in our implementation. *ChipletPart* with its core cost model is permissively open-sourced [11], enabling others to readily adapt it for benchmarking and further development. Also, we make our testcases publicly available, enabling the community to access a new, standardized set of benchmarks.

In the following, Section II reviews related works on chiplet cost modeling, partitioning and floorplanning. Sections III and V respectively provide an overview and details of our partitioning approach. Section IV describes the driving considerations in chiplet partitioning. Sections VI and VII show experimental results and additional case studies, and Section VIII concludes the paper.

## II. RELATED WORK

We now discuss fundamentals and previous works on chiplet cost modeling, then review existing works on chiplet partitioning and floorplanning. Tables I and II summarize key terms and notations.

### A. Chiplet Cost Modeling

Cost reduction is one of the main drivers for developing 2.5D systems. The total cost of developing a VLSI system

TABLE I: General terminology and notation.

Notation	Description
$\mathcal{C}$	Set of chiplets
$\mathcal{C}_t$	Set of chiplets implemented in technology node $t$
$N$	Chiplet-level netlist
$\mathcal{S}$	Block-level netlist
$V$	Chip manufacturing volume
$\mathcal{T}$	Set of technology nodes
$\omega$	Mapping from chiplets to technology nodes
$\phi$	Partitioning objective function
$m$	Number of different technology nodes

can be divided into two parts: non-recurring engineering (NRE) cost and recurring engineering (RE) cost [12]. NRE cost refers to the one-time cost of designing a VLSI system, including IP qualification, architecture, verification, physical design, software, etc. RE cost refers to the fabrication costs in mass production, such as wafers, packaging and testing. Researchers have proposed several chiplet cost models to estimate various components of the total 2.5D system cost. [12] introduces a quantitative cost model for comparing RE and NRE costs between monolithic SoC and multi-chip integration, but accounts for fewer RE cost considerations than our chosen model. [13] and [7] propose cost models that take into account reliability issues such as bump stress and warpage. [3], [9] presents a case study of a large system built using chiplets and analyzes the sensitivity of system cost to factors such as defect density, assembly cost, IO size, etc. The authors have made their cost model publicly available at [10]. In this work, we use the cost model proposed by [10] (see Section IV) due to the wide range of configurable parameters available for system technology co-optimization (STCO).<sup>2</sup> [9] was used in collaboration with IMEC to perform an STCO study in [14]. While the specific parameter settings in the cost model do influence partitioning outcomes, all parameters are externally configurable via user-defined configuration files. To enable efficient integration with our partitioning framework, we ported the cost model to C++, resulting in significantly improved performance.

### B. Chiplet Partitioning and Floorplanning

Several previous works address chiplet partitioning. [15] incorporates the min-cut partitioner *hMETIS* [16] within a chiplet implementation flow. [7] proposes *parChiplet*, which partitions the SoC system into chiplets based on functional and area characteristics of IP blocks. However, [15] [7] do not optimize the actual chiplets cost. *Chipletizer* [8] proposes a unified design characterization graph to represent both SoC designs and chiplets, and uses simulated annealing (SA) to optimize the overall cost

<sup>2</sup>To the best of our knowledge, the cost model in [10] is the most detailed open-source cost model currently available for chiplets.

TABLE II: GA terminology and notation. Default hyperparameters were empirically determined (Section VI-B4).

Notation	Description
$tot_{pop}$	#members in the population (default 50)
$k_{pop}$	Number of pairs of parents selected from a population for tournament selection (default 45)
$\zeta$	Tournament size (default 3)
$\sigma$	#members picked for elitism (default 5)
$\Delta_{threshold}$	Threshold value for improvement between successive generations (default 0.01)
$\Psi$	Maximum number of generations (default 50)
$\epsilon$	Maximum number of successive generations with cost improvement less than $\Delta_{threshold}$ (default 10)
$p_c$	Crossover probability (default 0.60)
$p_m$	Mutation probability (default 0.07)
$K_{max}$	Maximum number of attainable chiplets (default 8)

TABLE III: Comparison of chiplet partitioning methods.

Methods	Cost-Driven	Floorplan Feasibility	Heterogeneous Integration
[7], [15], [16]			
[8]	✓		
[17]	✓		✓
<i>ChipletPart</i>	✓	✓	✓

of chiplet-based systems. However, *Chipletizer* does not consider floorplan feasibility or heterogeneous integration. The recent work of [17] uses reinforcement learning (RL) and simulated annealing (SA) to perform PPA-oriented chiplet partitioning. However their method does not guarantee floorplan feasibility. The main differences between our *ChipletPart* and previous works are summarized in Table III. In our experimental evaluations, we compare *ChipletPart* with [16] and [7]. The authors of [15], [8] and [17] have not released their source code or binaries.<sup>3</sup>

Existing chiplet floorplanning approaches fall into three categories: simulated annealing (SA)-based, branch-and-bound (B&B)-based and mathematical programming (MP)-based. Works such as [18] [19] use classical floorplan representations such as B\* tree and apply SA to optimize an objective function. [20] [21] enumerate possible floorplanning solutions and apply B&B to find a near-optimal solution. [7] [13] develop MP-based formulations of chiplet floorplanning, enabling MP solvers to find optimal solutions. We note that existing works fail to handle the “reach” constraints imposed by IO cells, and generally assume that the size and shape of chiplets are predetermined by designers. Our present work proposes a reach-aware chiplet floorplanner, which simultaneously determines the location and shape for each chiplet.

### III. OUR APPROACH

We now introduce the chiplet partitioning problem, then give an overview of our chiplet partitioning framework.

<sup>3</sup>We contacted the authors of [17], but have not received netlists or explanations of their methodology, as had been expected.

#### A. Problem Formulation

Chiplet partitioning is fundamentally different from classical min-cut partitioning. The key differences are summarized as follows.

- **Problem size:** Min-cut partitioning is typically performed on gate-level netlists comprising millions of gates. By contrast, chiplet partitioning focuses on a block-level netlist that typically comprises several hundreds of IP blocks.
- **Objective:** Min-cut partitioning focuses on minimizing *cutsizes*, the number of nets (hyperedges) crossing partition boundaries. By contrast, chiplet partitioning seeks to reduce 2.5D system development cost, which brings a more complex set of considerations (Section IV).
- **Constraints:** Min-cut partitioning minimizes *cutsizes* subject to a given balance constraint [6]. By contrast, chiplet partitioning is not necessarily balanced, but it must produce *IO-feasible* solutions (Section V-B).
- **Heterogeneity:** Min-cut partitioning is insensitive to partition labels: swapping the contents of two partitions will not affect *cutsizes*. By contrast, chiplet partitioning is sensitive to partition labels (i.e., technology node assignments): swapping the technologies of two chiplets can significantly change total cost of a 2.5D system.

These fundamental differences between min-cut partitioning and chiplet partitioning motivate our studies. Formally, the inputs to our multi-technology chiplet partitioning framework are a block-level netlist  $\mathcal{S}$  and a set of technology nodes  $\mathcal{T}$ . The outputs are a set of chiplets  $\mathcal{C}$  and their corresponding technology assignment  $\omega : \mathcal{C} \rightarrow \mathcal{T}$ . The objective is to minimize the total cost of a 2.5D system:

$$\phi_{overall}(\mathcal{C}) = \frac{\phi_{assembly} + \sum \frac{\phi_{die}}{Y_{die}}}{Y_{assembly}} + \frac{g(\omega)}{V} \quad (1)$$

where  $\phi_{die}$  is the silicon cost of each chiplet,  $\phi_{assembly}$  is the assembly cost,  $Y_{die}$  is the die yield,  $Y_{assembly}$  is the assembly yield,  $g(\omega)$  is the non-recurring engineering cost, and  $V$  is the chip manufacturing volume. The constraint is the IO feasibility of the chiplet set  $\mathcal{C}$ .

#### B. Overview of ChipletPart Framework

We now describe our chiplet partitioning framework, *ChipletPart* (see Figure 2). Our *ChipletPart* differs from classical min-cut partitioners [4], [5], [6] and previous approaches [2], [8], [7], [15] in several key respects. (i) We optimize a comprehensive chiplet cost function (Section IV), unlike min-cut partitioners that focus on minimizing net *cutsizes*. (ii) We integrate a fast, Go-With-the-Winners [22] SA-based chiplet floorplanner to ensure IO-feasibility of each partitioning solution (Section V-B). (iii) We leverage a genetic algorithm (GA) framework to discover high-quality technology node assignments for heterogeneous integration.

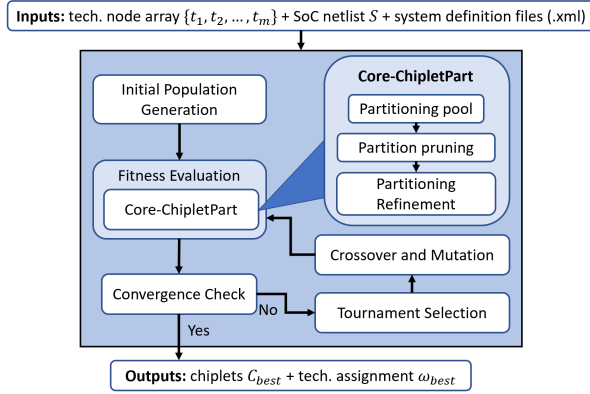


Fig. 2: *ChipletPart* Framework. *Core-ChipletPart* is shown in Figure 5. Partitioning refinement is shown in Figure 6.

*ChipletPart* inputs include a system block-level netlist  $S$ , a set of technology nodes  $\mathcal{T}$ , and system definition provided in XML files.<sup>4</sup> The algorithm is outlined in Algorithm 1 and visually illustrated in Figure 3. Within the GA framework, a *gene* is a technology node, and a *genome* is a sequence of technology nodes in which corresponding chiplets (partitions of  $S$ ) will be implemented. Details and source code for our GA-based partitioning and technology assignment methodology are in [11].

**Step 1: [Lines 3-4]** We first generate the initial population in the GA. Each member in the population (a *genome*) represents an ordered sequence of technology assignments (to chiplets)  $\omega : \mathcal{C} \rightarrow \mathcal{T}$ . We generate  $tot_{pop}$  ( $tot_{pop} = 50$  by default) genomes; each genome is generated by randomly mapping  $K_{max}$  chiplets to technology nodes  $\mathcal{T}$ .<sup>5</sup> To avoid redundant evaluations and improve scalability, we canonicalize all generated genomes by mapping functionally equivalent assignments to a unique representation. For example, genomes  $\langle 7nm, 7nm, 14nm \rangle$  and  $\langle 14nm, 7nm, 7nm \rangle$  are treated as equivalent, since they correspond to the same multiset of assignments.

**Step 2: [Lines 5-11]** We assess the fitness of each genome in the current population. For each genome  $\omega_j$ , we (i) run *Core-ChipletPart*<sup>6</sup> to generate a partitioning solution based on  $\omega_j$  and (ii) calculate the *fitness score* of this solution using our cost model.

**Step 3: [Lines 12-21]** We declare convergence if either of the following two termination criteria is met:

- The algorithm reaches the maximum number of generations,  $\Psi$  ( $\Psi = 50$  by default). Upon reaching this limit, the algorithm terminates and returns the best

<sup>4</sup>As in [3], [9], our netlists are modeled as graphs rather than hypergraphs, since these previous works use a directed (source-sink) edge for every inter-block connection.

<sup>5</sup>For simplicity, we set  $tot_{pop} = k_{pop} + \sigma$ .

<sup>6</sup>For better scalability, we run *Core-ChipletPart* with fewer FM (Fiducia–Mattheyses) moves and passes, and fewer initial solutions. Details are seen in our code [11].

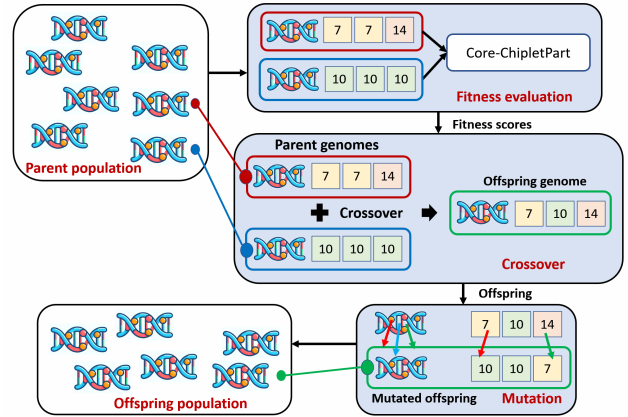


Fig. 3: GA-based technology assignment. A genome is a set of technology nodes. Shown: two parent genomes  $\langle 7, 7, 14 \rangle$  and  $\langle 10, 10, 10 \rangle$  undergo crossover to produce the offspring  $\langle 7, 10, 14 \rangle$ ; the offspring undergoes mutation to produce  $\langle 10, 10, 7 \rangle$  for the next-generation population.

chiplet solution,  $C_{best}$ , along with its corresponding technology mapping,  $\omega_{best}$ .

- The improvement between successive generations falls below a predefined threshold,  $\Delta_{threshold}$  ( $\Delta_{threshold} = 0.01$  by default), and remains below this threshold for more than  $\epsilon$  consecutive generations ( $\epsilon = 10$  by default). If this condition is met, the algorithm terminates and returns  $C_{best}$  and  $\omega_{best}$ .

**Step 4: [Line 22]** We use *tournament* selection [23] to identify candidate parents for crossover. Rather than evaluating the entire population at once, the selection process operates on randomly chosen “tournaments”, each consisting of  $\zeta$  genomes competing based on their fitness scores. The genome with the highest fitness in each tournament is selected as a candidate parent. This procedure is repeated until  $k_{pop}$  pairs of parents are chosen.<sup>7</sup>

**Step 5: [Lines 23-25]** We generate the next-generation population (offspring) through crossover, elitism, and mutation. Notably, we use uniform crossover [24] and random resetting mutation [25]. Additionally, we retain the top  $\sigma$  genomes from the parent generation based on their fitness scores (elitism), ensuring that high-quality solutions persist across generations.

In our implementation, we set  $tot_{pop} = 50$ ,  $\zeta = 3$ ,  $k_{pop} = 45$ ,  $\sigma = 5$  and  $K_{max} = 8$  (Section VI-B4). So, we conduct 90 tournaments (each tournament picks 3 genomes from the current generation) to select 90 parent genomes, which are then paired to generate 45 offspring genomes through crossover and mutation. We then supplement these 45 offspring with the top 5 genomes from the current generation (elitism), to generate the next generation population

<sup>7</sup>A genome can be selected multiple times as a parent.

of 50 genomes. For additional implementation details, we refer the reader to [11].

**Choice of optimizers:** Our choice of picking GA and SA is motivated by their ability to flexibly optimize over black-box, non-convex and highly discontinuous cost landscapes—characteristics inherent to our chiplet cost model (Section IV-A). In contrast, ILP-based methods are less suitable for our framework due to the lack of closed-form or linearizable expressions for IO feasibility and chiplet cost functions.<sup>8</sup> GA enables direct co-optimization of technology assignment and chiplet partitioning, while SA ensures that floorplanning solutions are always IO-feasible. Having a unified optimization approach with a unified formulation is challenging since the solution space spans both discrete combinatorial variables (chiplet-to-tech assignment) and continuous geometric constraints (IO reach), which are difficult to encode and optimize jointly. We hence opt for a modular decomposition—using GA for assignment and SA for feasibility evaluation.

In the following sections, we discuss the chiplet cost model, *Core-ChipletPart*, and the SA-based floorplanner.

#### IV. CHIPLET PARTITIONING DRIVERS

Smaller chiplets can potentially yield lower costs and improved yield, while technology heterogeneity offers better power and performance. The overhead of inter-chiplet IO also affects how a system should be partitioned into chiplets. In this section, we briefly discuss these factors.

##### A. Chiplet Cost Model

We use the open-source cost model from [9], [10]. It computes cost and yield based on the chiplet/interposer area (dependent on the technology node), assembly processes (dependent on bonding parameters), and IO placement constraints (dictated by netlist connectivity and reach). The model calculates the individual cost and yield of each chiplet along with the interposer, and then aggregates them for the full assembly cost. We consider designs as high volume in this case, to minimize the impact of NRE. The cost model is summarized by Equation 1. For further details, see [9]. Benefits of using the cost model in [9] are discussed in Section VI-B with results in Table V.

A block will have different areas and power in different technology nodes. While assigning a block to a more advanced technology node could, in principle, improve performance, we assume a fixed system architecture in this work and therefore hold performance constant while scaling power accordingly. Modeling architectural changes based on block-to-technology assignments is beyond the

<sup>8</sup>Exploring alternative combinatorial optimizers, such as Bayesian Optimization or Reinforcement Learning, is a promising direction for future work, particularly as surrogate models or parallel evaluation strategies can significantly improve runtime.

---

#### Algorithm 1: Overall *ChipletPart* framework.

---

**Input:** Standard Inputs:  $\mathcal{T}, \mathcal{S}$   
Hyperparameters:  $tot_{pop}, k_{pop}, \Delta_{threshold}, \epsilon, \zeta, \Psi, \sigma$   
**Output:** Chiplet partitioning solution  $C_{best}$ ,  
Technology assignment  $\omega_{best}$

```

1  $\Delta_{threshold} \leftarrow 0.01; \epsilon \leftarrow 10; \zeta \leftarrow 3; \Psi \leftarrow 50; \sigma \leftarrow 5;$ 
2  $tot_{pop} \leftarrow 50; k_{pop} \leftarrow 45; p_c \leftarrow 0.60; p_m \leftarrow 0.07;$ 
    $K_{max} \leftarrow 8;$ 
   /* 1. Initial population generation */
3  $Cost_{best} \leftarrow \infty; Cost_{prev} \leftarrow \infty; \Delta \leftarrow \infty;$ 
4 Generate the initial population with  $tot_{pop}$  genomes where
   each genome is a random mapping from  $K_{max}$  chiplets to  $\mathcal{T}$ ;
5  $i \leftarrow 0; num\_iters \leftarrow 0$ 
6 while true do
   /* 2. Fitness evaluation */
7   foreach  $\omega_j$  in the current population do
8      $C_{\omega_j} \leftarrow$  Generate the partitioning solution using
       Core-ChipletPart with technology assignment  $\omega_j$ ;
9      $Cost_{\omega_j} \leftarrow$  Calculate the cost of  $C_{\omega_j}$  (Section IV);
10    if  $Cost_{\omega_j} \leq Cost_{best}$  then
11       $Cost_{best} \leftarrow Cost_{\omega_j}; C_{best} \leftarrow C_{\omega_j};$ 
        $\omega_{best} \leftarrow \omega_j;$ 
   /* 3. Convergence check */
12  if  $num\_iters \geq \Psi$  then
13    return  $C_{best}, \omega_{best}$ 
14   $\Delta \leftarrow Cost_{prev} - Cost_{best};$ 
15  if  $\Delta \leq \Delta_{threshold}$  then
16     $i \leftarrow i + 1;$ 
17    if  $i > \epsilon$  then
18      return  $C_{best}, \omega_{best}$ 
19  else
20     $i \leftarrow 0;$ 
21   $Cost_{prev} \leftarrow Cost_{best};$ 
   /* 4. Tournament selection */
22  Select  $k_{pop}$  pairs of parents using tournament selection
   with tournament size  $\zeta$ ;
   /* 5. Crossover, elitism and mutation */
23  Perform crossover on each selected pair  $(\omega_x^p, \omega_y^p)$  to
   generate offspring  $\omega_x^o$ , using a crossover probability  $p_c$ ;
24  Apply mutation to each offspring  $\omega_x^o$  with mutation
   probability  $p_m$ ;
25  Construct the next generation by selecting the top  $\sigma$  elite
   genomes from the current generation, along with  $k_{pop}$ 
   offsprings;
```

---

scope of the current work and is left as a future direction. We follow [26] to model this scaling. Different technology nodes result in different cost per unit area for chiplets, along with differences in yield and reticle-fit dependent lithography costs [9]. We also scale memory and logic with different factors [27] since memory tends to scale poorly for advanced nodes. Different technology nodes will also have different non-recurring design [28] and manufacturing costs [29]. For example, the transition between 45nm and 10nm reduces logic size by a factor of  $\sim 10\times$  [26], while NRE design cost increases by  $\sim 4.6\times$  [28] and general cost per wafer increases by  $\sim 2.6\times$  [30].

##### B. Chiplet Power Model

We assume that performance of chiplets is preserved across technology nodes but that the power changes. We further assume that inter-chiplet communication latency is small enough to not influence the architecture. If certain

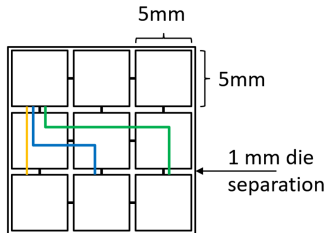


Fig. 4: Illustration of *reach*. Wirelengths: black - 1 mm, orange - 7 mm, blue - 13 mm, and green - 19 mm.

inter-block interfaces are highly latency-sensitive, then those blocks should be merged in our framework so as to map them to the same chiplet. More complex performance models as in [7] are possible but not explored in this work.

Power is calculated as the sum of block power and IO power. If all blocks are in the same chiplet, there will be no additional power due to IO. However, if the blocks are placed into multiple partitions (chiplets), some additional power will be consumed by the added IO cells. We scale the block power according to the scaling factors in [26] for different technology nodes.

### C. IO Reach Model

We use an IO cell model where each IO cell has both an area and a “reach” which is the maximum wire length that can be driven by the IO cell. The reach depends on the IO transceiver design and is often dictated by the inter-chiplet IO standard. E.g., Universal Chiplet Interconnect Express (UCIe) [31] guarantees a UCIe reach of 2mm for advanced packages while standard packages (such as organic substrates) support larger reaches of up to 25mm.

Since we assume a fixed system architecture, our partitioner does not modify the network structure or insert pipeline stages to compensate for long inter-chiplet wires. We also assume a standardized IO cell with a fixed maximum reach instead of more complicated IO structures. These assumptions help keep the partitioning problem well-scoped and tractable. We leave sophisticated IO planning including pass-through connections, inserting buffers on the substrate, multiple IO types per design, etc. to future work. However, users can explore multiple architectural variants and IO types for the same design. For example, in our industry testcase (Section VI-A), we evaluate two versions that differ only in their crossbar configurations—and in Figure 13, we examine the impact of different IO cell types on partitioning.

Consider the example in Figure 4, and assume that a bundle of wires is connected from the side of one chiplet to the side of another. If the chiplets are 5mm on a side and spaced apart by 1mm, then the short black connections require a reach of at least 1mm, while the orange/blue/green connections respectively require reach of at least

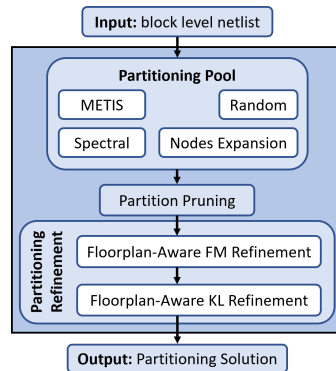


Fig. 5: *Core-ChipletPart* partitioning flow. We use multiple techniques shown in the partitioning pool to generate the initial partitions, then we prune out the worst-performing initializations before running refinement.

7mm/13mm/19mm. Small values of reach constrain the floorplan, while larger values of reach come at the cost of more expensive IO cells.

IOs are discretized depending on the standard. For instance, a single UCIe IO cell is as large as  $0.88 \text{ mm}^2$  [31] while for parallel signaling (e.g., AIB or [32]), an IO cell can be as small as  $157 \mu\text{m}^2$  [33]. This discretization can cause complexity for chiplet partitioning, as the IO (i.e., net cut) cost calculation follows a staircase-like curve as a function of net cut.

## V. CHIPLET PARTITIONING CORE

In this section, we first discuss our chiplet-cost-driven partitioning approach *ChipletPart-Core* in Section V-A. Then, we present our reach-aware chiplet floorplanning approach in Section V-B.

### A. Cost-driven Partitioning: *Core-ChipletPart*

Our *Core-ChipletPart* does not adopt the widely-used multilevel approach since there are typically only a few hundreds of IP blocks in a block-level netlist. As shown in Figure 5, we (i) compute a large pool of initial partitioning solutions using a variety of graph partitioning algorithms; (ii) prune poor-quality partitioning solutions from the pool; and (iii) perform floorplan-aware Fiducial–Mattheyses [34] (FM)-based and Kernighan–Lin [35] (KL) refinement. We then output the solution with the best cost.

**Generation of a partitioning pool.** Similar to the initial partitioning stage in widely used multilevel partitioning approaches [4] [6], we compute a pool of initial partitioning solutions so as to explore a larger solution space.<sup>9</sup> Specifically, we use the following graph partitioning methods.

<sup>9</sup>However, unlike multilevel approaches [4] [6], *Core-ChipletPart* omits the coarsening stage due to the relatively small number of vertices (i.e., 384 IP blocks in our largest testcase, as shown in Table IV).

- *Spectral partitioning*: Because the block-level netlist is both small and sparse, we apply *spectral partitioning* [36]. We first compute the spectral embedding using the two smallest nontrivial eigenvectors, then cluster the IP blocks with the K-means algorithm [37].<sup>10</sup>
- *High degree nodes expansion*: Our node expansion approach follows [39]. In the block-level netlist, high-degree nodes (e.g., crossbars) are distributed across different chiplets, and then expanded via breadth-first search. If multiple chiplets qualify for expansion, the block is assigned to the chiplet with which it has the strongest connection.
- *Random partitioning*: We randomly distribute all blocks across different chiplets. We generate multiple random solutions while sweeping  $K = \{1, \dots, K_{\max}\}$ .<sup>11</sup> We consider  $K = 1$  to allow the degenerate case where all the blocks are placed in a single chiplet.
- *METIS*: We use the METIS graph partitioner [16] to create initial partitioning solutions, using the METIS APIs from [40]. Similar to our random partitioning approach, we sweep  $K = \{2, \dots, K_{\max}\}$ .

Our partitioning pool consists of 11 solutions in total: one from the spectral method, one from node expansion, five from random partitioning, and four from METIS. We next discuss the pruning step, which discards low-quality solutions from this pool.

**Partitioning solution pruning.** We use a statistical filtering mechanism to prune the partitioning pool. First, we compute the cost of each initial partition using our cost model (Section IV-A), and then calculate the mean and standard deviation of these costs, as well as each partition’s cost relative to the best solution. Our pruning applies two complementary thresholds: (i) a Z-score [41] threshold, eliminating partitions whose costs exceed 1.5 standard deviations above the mean and (ii) a relative cost threshold, removing partitions whose costs are worse than twice the minimum cost. To prevent over-pruning, we retain at least three solutions even if they all appear statistically poor. Pruning significantly reduces computational workload by eliminating low-quality candidates early.

**Partitioning refinement.** We use two different refinement strategies for refinement: (i) FM and (ii) KL. Both these processes are shown in Figure 6. Each potential FM move or KL pair swap triggers a call to the chiplet cost model to obtain the cost (gain) of an updated partitioning solution. This evaluation includes generating a floorplan solution using the “fast” mode of our SA-based reach-aware chiplet floorplanner, followed by calculating the corresponding cost. After completing each FM or KL pass, the “standard”

<sup>10</sup>In our implementation, we use a parallel K-means method with smart initialization (K-means++ [38]), and we set  $K = 4$  by default.

<sup>11</sup>Our studies show that  $K_{\max} = 8$  is sufficient for our testcases. If the solution finds  $K_{\max}$  number of partitions, the user can increase  $K_{\max}$  to check larger numbers of partitions.

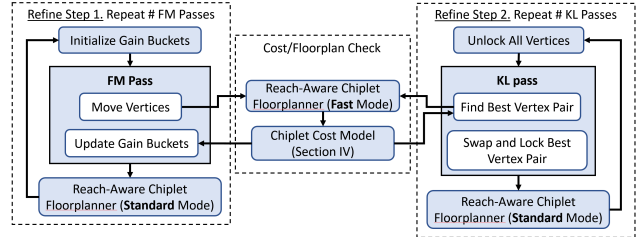


Fig. 6: Floorplan-aware FM and KL-based refinement. In our implementation, we first run FM followed by KL.

mode of the SA-based reach-aware chiplet floorplanner is employed to search for an improved floorplan solution for the subsequent pass. Further details about our SA-based reach-aware chiplet floorplanner are provided in Section V-B. We adopt the K-way FM implementation from *TritonPart* [6], while our KL refinement [42] follows the methodology described in [35]. In our implementation, we apply KL after FM to further improve solution quality, as KL explores a broader neighborhood by enabling pairwise vertex swaps—compared to FM’s single-vertex moves.

### B. Reach-aware Chiplet Floorplanning

Chiplet floorplanning is a crucial step, as it determines the location and shape of each chiplet on the interposer. In contrast to the well-studied macro placement, chiplet floorplanning must also consider IO feasibility. More specifically, the wirelength of a net must not exceed the reach specified by the corresponding IO cell (Section IV). Figure 7 illustrates the wirelength (measured in terms of Manhattan distance) calculation for net  $e$  connecting chiplets  $A$  and  $B$ . Assuming that the bitwidth of net  $e$  is  $n_e$  and the area of IO cells is  $A_{IO}$ , then the wirelength of net  $e$  ( $length(e)$ ) in the figure is calculated as: (i)  $l = \sqrt{w^2 + 2A_{IO}} - w$  and (ii)  $length(e) = h + 2l$ , where  $l$  is the depth needed for all the IO cells.<sup>12</sup> Then the reach violation penalty for net  $e$  is  $n_e \times \max(length(e) - reach(e), 0.0)$ . The reach violation penalty for a chiplet is defined as the summation of the reach violation penalties for all the nets connected to the chiplet.

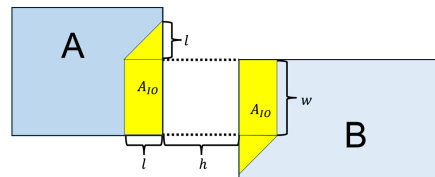


Fig. 7: Illustration of wirelength computation ( $length(e)$ ). The yellow region indicates the placement area for IO cells that will satisfy the reach constraint.

**Problem formulation.** Our work uses a novel reach-aware chiplet floorplanning approach. The input to our

<sup>12</sup>The detailed code for more general cases is available in [43].

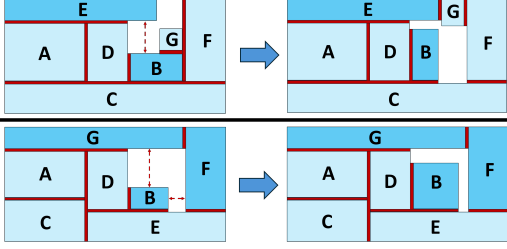


Fig. 8: Top: Resizing of chiplet B fixes a reach violation for a net connecting chiplets B-E. Bottom: Expansion (bloating) of chiplet B fixes reach violations for nets connecting chiplets B-G and B-F. In each figure pair, left = before; right = after. Red regions indicate the separation constraint between chiplets, and red dashed arrows indicate reach violations before fixing.

floorplanner is a set of chiplets  $C$ , and a chiplet-level netlist  $\mathcal{N}$  that defines the connections between chiplets. The output is a floorplanning solution which provides the location and shape (width and height) of each chiplet. The objective of our floorplanner is

$$WL_{reach} = \sum_{e \in \mathcal{N}} n_e \times \max(\text{length}(e) - \text{reach}(e), 0.0) \quad (2)$$

$$\min \quad \alpha \times WL_{reach} + \beta \times A_C + \gamma \times A_P \quad (3)$$

where  $WL_{reach}$  represents the reach violation penalty,  $A_C$  represents the area of chiplets, and  $A_P$  represents the area of the package.  $\alpha$ ,  $\beta$  and  $\gamma$  are user-defined coefficients that can be modified to achieve a desired tradeoff between multiple objectives.<sup>13</sup> Note that we allow the area of chiplets to increase to satisfy the reach constraints. During optimization, the following constraints are considered:

- **Overlap constraint:** No two chiplets can overlap.
- **Separation constraint:** In practical chiplet-based systems, extra space must exist between neighboring chiplets to account for dicing and alignment accuracy, and to prevent defects and mechanical stress during chiplet assembly. The separation constraint sets the minimum distance between any two chiplets.

**SA-based chiplet floorplanner.** Our reach-aware floorplanner uses Sequence Pair [44] to represent spatial arrangement of chiplets in the netlist and Simulated Annealing [45] to optimize the objective function. The Sequence Pair-based annealing supports five solution perturbation (move) operators with respective probabilities 0.2, 0.2, 0.2, 0.2 and 0.2:

- **Op1:** Swap two chiplets in the first sequence.
- **Op2:** Swap two chiplets in the second sequence.
- **Op3:** Swap two chiplets in both sequences.
- **Op4:** Reshape a chiplet. Find the chiplet with highest reach violation penalty and change its shape using the

<sup>13</sup>The default values for  $\alpha$ ,  $\beta$  and  $\gamma$  are 1.0, 1.0 and 1.0, respectively.

resizing algorithm in [46]. The example of Figure 8 (top) shows how a reach violation for the net connecting chiplets E and B (red dashed arrow) is fixed by aligning the right boundary of B with the right boundary of E.

- **Op5:** Expand (i.e., bloat) a chiplet. Find the chiplet with highest reach violation penalty and bloat it to occupy neighboring whitespace, with bloating in each direction determined by the length required to fix the reach violation. Figure 8 (bottom) shows how reach violations for nets connecting chiplets B-G and B-F are fixed by bloating B towards the top and right. This operator helps reduce the reach violation penalty but comes at the expense of increasing both the chiplet area and the overall package area.

To enhance the performance of simulated annealing (SA), we adopt a *Go-With-the-Winners* (GWTW) strategy [22], which enables 10 parallel SA *walkers* to independently explore the solution space. Periodically, a synchronization phase is performed in which: (i) the best-performing threads are identified, (ii) their solutions are cloned to repopulate the thread pool and (iii) all threads resume independent exploration. This strategy balances diversification and intensification, improving convergence without incurring significant runtime overhead. We use 10 threads in our experiments, a setting that is easily supported on standard server-class machines.<sup>14</sup> As discussed in Section V-A, our chiplet floorplanner operates in two modes: “standard” and “fast”. The standard mode performs 1,000,000 perturbations with a cooling rate of 0.989, while the fast mode performs 10,000 perturbations with an initial temperature of 0.0 (greedy). In our experiments, the “standard mode” is invoked after each FM or KL pass (default: 4 passes), totaling four invocations per run. The fast mode is triggered after each FM vertex move (default: 50% of all vertices) and each KL vertex swap (default: 10% of all vertices), resulting in 230 invocations per pass in our largest testcase. These parameters were empirically selected to strike a balance between runtime and solution quality.

## VI. EXPERIMENTAL RESULTS

*ChipletPart* is implemented using approximately 27K lines of C++ code, building upon implementations from [6]. We use OpenMP [47] for parallelization, the Eigen library [48] for spectral partitioning, codes from [40] to run METIS and Boost [49] for high precision arithmetic computations in the cost model. Additionally, we have translated the Python-based cost model from [9], [10] into C++ and integrated it into our *ChipletPart* framework. The scripts and source code of *ChipletPart*, including its cost model implementation, are available in [11]. We run all

<sup>14</sup>This number of threads is typical for modern multi-core servers and does not impose a significant hardware burden.

experiments on a Linux server with Intel Xeon E5-2690 CPU (48 threads) and 256GB RAM.

### A. Benchmarks and Baselines

We evaluate four categories of testcases in this work: Waferscale, MemPool, Industrial Testcase and Comparison Testcases. A common issue in partitioning research is that most testcases are too small to warrant practical chiplet partitioning; existing works often focus on very small designs, overemphasizing the impact of IO and underemphasizing yield and packaging costs. To address this, we scale up the power and area of our baseline designs to sizes more representative of real commercial systems (e.g., Intel’s Ponte Vecchio [1]). We also scale the interconnects using Rent’s Rule,<sup>15</sup> applying constants from [51] for microprocessor and memory blocks. This ensures that our scaled designs have a realistic number of IOs, making them suitable for evaluating chiplet partitioning.

Our first category of testcases (*Waferscale*) is derived from the waferscale graph processor in [32]. We extract synthesized IP block areas and a block-level netlist at 45 nm, then apply area and power scaling to favor partitioning. The second category (*MemPool*) is similarly extracted from synthesized blocks in [52] and likewise scaled from its 45 nm block-level netlist. The third category (*Industry Testcase*) is based on a 16nm design provided by a semiconductor company, which we also scale to a suitable size. Finally, the *Comparison Testcases* based on publicly available information for large commercial designs come from [8]. The original implementations were in various nodes and these designs are sufficiently large that they do not require further scaling.

Table IV shows the specific testcase configurations that we use; see also the design-specific discussion below. In the table, the *WS* testcases are based on the *Waferscale* design, the *MP* testcase is based on the *MemPool* design, the *TC* testcase is based on the *Industry* design and *EPYC* and *GA100* are the *Comparison Testcases*. The specific parameters are explained as follows.

**Waferscale Testcases.** The waferscale design is organized into a grid of tiles connected in a 2D mesh configuration with neighbor-to-neighbor communication between tiles. Each tile comprises 48 IP blocks. Those blocks include a router for tile-to-tile connections, a crossbar for intra-tile connections, 4 large shared memory blocks connected to the crossbar, and 14 cores each with associated bus and private memory blocks. Figure 9 gives a system block diagram. We have implemented a testcase generator (see [11]) which allows us to choose the number of tiles in a given testcase, along with the number of cores and memories per tile. Area and power scaling are also provided

<sup>15</sup>Rent’s Rule [50] states that the number of terminals  $T$  in a logic block scales as  $T = kC^p$ , where  $k$  is a constant,  $C$  is the number of components and  $p$  is the Rent parameter. Hence, if  $C$  is scaled by a factor  $s$ ,  $T$  is scaled by  $s^p$ .

TABLE IV: Benchmark characteristics. Note that MP and WS both use tile terminology; the others do not.

Benchmark	# Tiles	# IP Blocks	Area ( $mm^2$ )	Area Scaling	Power Scaling
WS <sub>1</sub>	1	48	1582 (45nm)	1600	1600
WS <sub>2</sub>	2	96	3165 (45nm)	1600	1600
WS <sub>3</sub>	4	192	6330 (45nm)	1600	1600
WS <sub>4</sub>	8	384	12,660 (45nm)	1600	1600
MP	16	40	494 (45nm)	100	100
TC <sub>1</sub>	N/A	14	567 (16nm)	16	16
TC <sub>2</sub>	N/A	17	567 (16nm)	16	16
EPYC	N/A	32	148 (7nm)	1	1
GA100	N/A	180	548 (7nm)	1	1

via the testcase generator. As noted, Table IV shows the waferscale configurations used in our case studies.

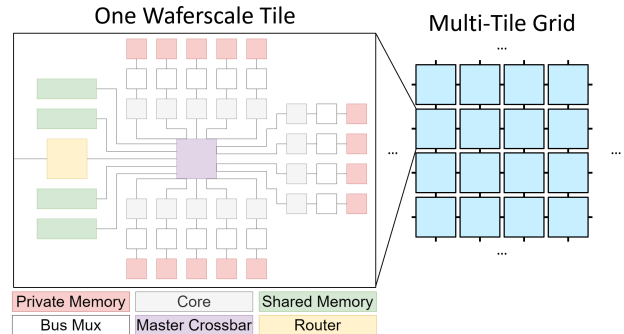


Fig. 9: Waferscale testcase. Left: example IP blocks in a tile. Right: Connection of tiles in a grid. This testcase allows scaling of the number of tiles to match a target design size for partitioning.

**MemPool Testcase.** The full MemPool design consists of 4 MemPool *groups*, each containing 16 MemPool *tiles*. These tiles each consist of cores and memory along with supporting logic. Note that while each tile contains 4 cores and 16 memory banks, we do not split tiles for partitioning. For our MemPool testcase, we use a single MemPool group, i.e., taken at just above the tile level of the hierarchy. Based on 16 tiles and 24 blocks related to (remote, local, AXI etc.) interconnect, our block-level netlist for MemPool group has 40 IP blocks to use in partitioning. A diagram is available in [11]; see also Figure 3(a) in [52].

**Industry Testcases.** We use a chip design from industry with parameters shown in Table IV.<sup>16</sup> Because the original design is relatively small, we scale the area and interconnect via Rent’s Rule to reach an overall design area of more than 400  $mm^2$ . This architecture follows a controller-target structure around a crossbar, where the crossbar constitutes 30% of the total area of its connected blocks.

**Comparison Testcases.** We also evaluate on two commercial designs used by Chipletizer [8]. The first is based on AMD’s EPYC 7282 [54], shown in Figure 10. We additionally examine NVIDIA’s GA100 chip [55], which

<sup>16</sup>The industry testcases are generated based on discussions with Analog Devices engineers [53].

TABLE V: Partitioning Results for hMETIS, TritonPart, FloorPlet [7], Manual, and ChipletPart. ChipletPart No-FP has no floorplan checker. “Feas” indicates IO-feasibility (✓: feasible, X: not feasible). Best (feasible) cost is in bold.

Benchmark	hMETIS			TritonPart			FloorPlet			Manual			ChipletPart No-FP			ChipletPart		
	C	Cost	Feas	C	Cost	Feas	C	Cost	Feas	C	Cost	Feas	C	Cost	Feas	C	Cost	Feas
WS <sub>1</sub>	5	72.4	X	3	77.3	✓	6	55.5	X	1	71.2	✓	7	55.1	X	6	<b>53.9</b>	✓
WS <sub>2</sub>	8	138.1	X	7	143.2	X	4	150.3	✓	2	145.5	✓	6	122.3	X	8	<b>123.4</b>	✓
WS <sub>3</sub>	7	316.3	X	8	362.4	X	4	310.5	✓	4	310.5	✓	8	319.6	X	7	<b>300.4</b>	✓
WS <sub>4</sub>	8	1449.5	X	8	1564.2	X	5	1237.9	X	8	674.3	✓	7	776.2	X	8	<b>659.9</b>	✓
MP	1	5.7	✓	1	5.7	✓	1	5.7	✓	1	5.7	✓	1	5.7	✓	1	<b>5.7</b>	✓
TC <sub>1</sub>	3	72.6	✓	3	68.1	✓	6	45.6	X	1	70.5	✓	4	47.2	✓	6	<b>46.5</b>	✓
TC <sub>2</sub>	3	73.9	✓	3	71.1	✓	7	46.5	X	4	49.4	✓	6	48.7	X	7	<b>46.2</b>	✓
EPYC	4	92.1	✓	4	96.3	✓	4	89.3	✓	4	80.8	✓	8	76.1	X	8	<b>72.5</b>	✓
GA100	3	52.3	✓	3	60.5	✓	2	42.1	✓	5	36.1	✓	2	33.6	✓	5	<b>31.8</b>	✓

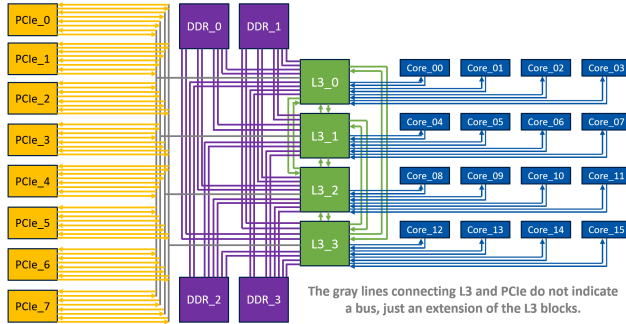


Fig. 10: AMD EPYC 7282 Testcase used in [8].

powers the A100 GPU. The GA100 design includes 128 simultaneous multiprocessor blocks, 40 L2 blocks and multiple HBM controller blocks, totaling 180 blocks. We omit the GA100 block diagram due to its size.

**Metrics.** For simplicity, we assume iso-performance for our testcases, even across technology nodes; instead, we derive advantages in power from improvements in IO count or changes in technology node. We also assume that connections between blocks in a chiplet will have the same speed as inter-chiplet connections, although the inter-chiplet connections will have higher power and area requirements due to large IO drivers. Design area is a major contributor to cost, and chip power also contributes to chip cost via added bumps (for current delivery) that require additional area. Given this, we use cost as a single metric for partitioning.

**Baselines.** Since there is no open-source, cost-driven chiplet partitioner available, we compare against: (i) *Min-cut partitioners* (hMETIS [16], which is often used in chiplet flows [15], and TritonPart [6]) applied to weighted hypergraphs, where each hyperedge is weighted by the corresponding I/O bandwidth; (ii) the *parChiplet* method from FloorPlet [7]; and (iii) partitioning solutions generated by human engineers.<sup>17</sup>

<sup>17</sup>Our attempts to contact the authors of [17] were unsuccessful. We are currently in correspondence with the authors of [8], but have encountered difficulties running their implementation. Efforts to resolve these issues are ongoing.

## B. Validations of Chiplet Partitioning

Given that previous works use traditional min-cut partitioners in 2.5D flows, we directly compare *ChipletPart* with leading partitioners *hMETIS* and *TritonPart*. We also compare to the *Floorplet* floorplan-aware chiplet partitioner [7] and *manual* partitions. For the *waferscale* testcases based on [32] we compare the memory-compute partition in that work with a per-tile partitioning as the manual partition. Overall, our validations span (i) validation of chiplet cost-driven partitioning, (ii) validation of floorplan-awareness, (iii) validation of heterogeneous technology-awareness, and (iv) analyses of hyperparameter sensitivities and runtime.

### 1) Validation of chiplet cost-driven partitioning

We evaluate *ChipletPart* against the baselines listed in the previous section: *hMETIS*, *TritonPart*, *FloorPlet* and manually derived partitions. Our validation is thus divided into three parts, detailed below.

**Comparison with netlist partitioners.** We evaluate the chiplet cost-driven partitioning capabilities of *ChipletPart* by benchmarking against leading netlist partitioners *hMETIS* and *TritonPart*, using the latter’s default parameter settings.<sup>18</sup> We use the testcases listed in Table IV for our evaluations, with results presented in Table V. For both *hMETIS* and *TritonPart*:

- We set an imbalance factor of 5%, and define our input set of partitions as  $K = 1, 2, 3, \dots, 10$ .
- For each  $K$ , we execute ten runs of the partitioner, yielding a total of 100 partitioning solutions.<sup>19</sup>
- We evaluate each partitioning solution using our cost model (Secs. IV and IV-B), and report the solution with lowest chiplet cost.
- Since *hMETIS* and *TritonPart* are not technology-aware, for a fair comparison, we enforce homogeneity by running *ChipletPart* with only the 7nm technology node.

<sup>18</sup>For *hMETIS*, the default settings are  $N_{runs} = 10$ ,  $CType = 1$ ,  $RType = 1$ ,  $Vcycle = 1$ ,  $Reconst = 0$ , and  $seed = 0$  [4]. For *TritonPart*, the default parameter settings are  $thr\_coarsen\_hyperedge\_size\_skip = 200$ ,  $coarsening\_ratio = 1.6$ ,  $max\_moves = 60$ , and  $num\_coarsen\_solutions = 3$  [6].

<sup>19</sup>Our studies show that longer partitioner runs do not improve the quality of results.

Consequently, the cost model evaluates all partitioning solutions using the 7nm technology node. The floorplanner is run in the standard mode (Section V-B).

Results are presented in Table V. Columns  $|C|$ ,  $Cost$ , and  $Feas$  respectively indicate the number of chiplets, the evaluated cost of the chiplet solution, and whether the solution satisfies the reach constraints. *ChipletPart* consistently produces solutions with better cost than *hMETIS* and *TritonPart*, with improvements of up to 55% and 58%, respectively. The geometric mean improvements over *hMETIS* and *TritonPart* are 16% and 20%, respectively. This result shows the advantages of *ChipletPart*'s cost-driven partitioning over traditional min-cut partitioners. Furthermore, *ChipletPart* consistently produces floorplan-feasible solutions, whereas standard netlist partitioners often fail to meet the reach constraints.<sup>20</sup>

**Comparison with previous work.** We compare *ChipletPart* with the *parChiplet* partitioner from *FloorPlet* [7]. Here, we set the *FloorPlet* parameters as  $|C|_{\min} = 1$ ,  $|C|_{\max} = 10$  and  $rr = 1.0$ . All partitioning solutions are evaluated using our cost model with the 7nm technology node and the floorplanner is run in standard mode. Table V presents these results. Compared to *FloorPlet*, *ChipletPart* achieves up to a 47% cost improvement, with a geometric mean improvement of 6%. While *FloorPlet* produces a solution with slightly lower cost on the  $TC_1$  testcase, the solution violates reach constraints. In contrast, *ChipletPart* consistently generates floorplan-feasible solutions with better cost, highlighting its strength in delivering high-quality and physically realizable chiplet partitions.

**Comparison with human baselines.** We generate human baselines for each testcase as follows. For the *Waferscale* ( $WS_1, WS_2, WS_3, WS_4$ ) designs, which are tile-based, the human partitioning solution aligns directly with these tiles. For the *Industry* testcases, we split around the crossbar;  $TC_1$  is a single partition and  $TC_2$  is a 4-way partition with the same blocks as  $TC_1$  but with a 4-way split crossbar. For the *EPYC* testcase (Figure 10), we cluster each set of cores with its corresponding L3—distributing other blocks to maintain regularity and balanced area—resulting in four partitions each containing 2 PCIe blocks, 1 DDR, 1 L3, and 4 cores. Similarly, for *GA100*, we create five chiplets: four partitions each holding 32 simultaneous multiprocessors and 10 L2 blocks, and one partition for the remaining blocks.<sup>21</sup>

Similar to the previous sections, all partitioning solutions are evaluated using our cost model with the 7nm technology node and the floorplanner is run in standard mode. Table V presents the results. *ChipletPart* generates

solutions that are up to 24% better than the manual baselines with a geometric mean improvement of 7%. While the human baselines are all floorplan-feasible, they are significantly suboptimal. We see that a black-box partitioner such as *ChipletPart* can find better-quality solutions compared to manual strategies.

### 2) Validation of floorplan-awareness

We also evaluate the impact of floorplan-awareness in *ChipletPart*. Table V compares solutions generated with and without floorplan-awareness enabled. Disabling floorplan-awareness can result in lower nominal chiplet costs ( $WS_2$ ), but frequently produces solutions that violate interconnect reach constraints. In fact, six out of nine testcases produce infeasible solutions when floorplan-awareness is disabled. In addition to feasibility, floorplan-awareness leads to up to 15% improvement in chiplet cost, with a geometric mean improvement of 4%. This is because our cost model incorporates floorplan-level information when evaluating partition quality—thus, floorplan-aware solutions better align with the true cost objective. These observations highlight the importance of incorporating floorplan-awareness: while it may slightly increase nominal cost in some cases, it helps to ensure that all generated solutions are physically realizable.

### 3) Validation of heterogeneous technology-awareness

We evaluate benefits of incorporating heterogeneous technology awareness on all nine testcases (Table IV) and a technology list comprising 14nm, 10nm, and 7nm nodes. Table VI shows chiplet cost reductions achieved through technology awareness relative to the best solutions obtained via homogeneous technology integration, for each technology node. We first run *ChipletPart* using a single technology node per testcase (homogeneous integration) to obtain partitioning solutions for each technology. We then run *ChipletPart* with technology awareness enabled (i.e., leveraging all three technology nodes) and compare the results. Our results show that heterogeneous technology assignment can reduce chiplet cost by up to 43%, with geometric mean cost reductions of 7%, 15%, and 15% when compared against homogeneous solutions at 7nm, 10nm, and 14nm, respectively.<sup>22</sup> Note, that all solutions generated by *ChipletPart* are floorplan feasible.

### 4) Hyperparameter exploration and sensitivity analysis

*ChipletPart* relies on four key hyperparameters for its genetic algorithm (GA): (i) total population size  $tot_{pop}$ ; (ii) maximum number of generations  $\Psi$ ; (iii) mutation probability  $p_m$ ; and (iv) crossover probability  $p_c$  (cf. Algorithm 1).<sup>23</sup> We validate the default values of these

<sup>20</sup>*hMETIS* and *TritonPart* optimize cutsize and return partitions with better cutsize compared to *ChipletPart* (albeit with worse chiplet cost).

<sup>21</sup>Our human baselines do not necessarily reflect partitions chosen by industry. Instead, we split the blocks to generate relatively even partitions with small cutset and high regularity as an example of what the human engineer might decide to do.

<sup>22</sup>To further validate the effectiveness of our GA, we implemented an enumeration-based framework that exhaustively explores all  $\sum_{k=1}^{K_{\max}} \binom{k+m-1}{m-1}$  possible assignments. Our experiments show that the GA achieves up to  $7\times$  speedup with less than 1% degradation in chiplet cost compared to the enumeration-based framework.

<sup>23</sup>*ChipletPart* never returns a chiplet solution with more than 8 chiplets, so we set  $K_{\max}$  to 8.

TABLE VI: Impact of heterogeneity. “Homogeneous” denotes homogeneous integration cost. “Heterogeneous” denotes heterogeneous integration cost, chiplet tech distribution, and *ChipletPart* runtime. A single invocation of *Core-ChipletPart*’s runtime is  $\sim 5\%$  of *ChipletPart*’s runtime.

Bench.	Homogeneous			Heterogeneous				
	7nm	10nm	14nm	Cost	#7nm	#10nm	#14nm	Runtime (s)
WS <sub>1</sub>	53.9	48.9	42.1	<b>41.7</b>	2	0	4	401
WS <sub>2</sub>	123.4	112.7	109.4	<b>87.8</b>	1	0	7	1421
WS <sub>3</sub>	300.4	310.4	286.3	<b>254.4</b>	3	0	5	3240
WS <sub>4</sub>	659.9	662.4	676.1	<b>656.2</b>	7	1	0	5624
MP	5.7	6.9	8.8	<b>5.7</b>	1	0	0	180
TC <sub>1</sub>	46.5	52.4	56.4	<b>39.8</b>	3	0	2	160
TC <sub>2</sub>	46.2	54.2	64.1	<b>39.3</b>	4	0	2	89
EPYC	72.5	86.2	94.6	<b>65.1</b>	3	0	2	349
GA100	31.8	40.5	55.2	<b>31.6</b>	3	1	0	493

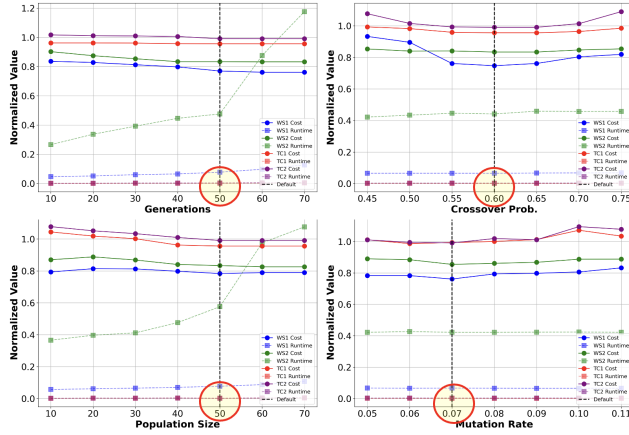


Fig. 11: Hyperparameters sweep across benchmarks. Solid lines denote normalized cost and dashed lines denote normalized runtime. The default hyperparameter choice is marked with a vertical dashed line and circled.

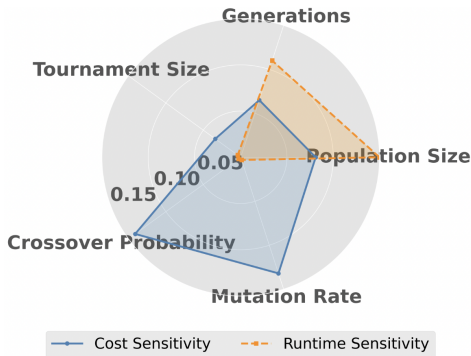


Fig. 12: Sensitivity analysis of hyperparameters. Larger (distance from plot center) indicate greater influence.

TABLE VII: Runtime breakdown of *ChipletPart*.

Component	Runtime share (%)
SA-based floorplanner	67
Partition refinement (chiplet cost model)	28
Partition pool	2
Partition pruning	1
I/O	1

hyperparameters via an empirical study using testcases  $WS_1$ ,  $WS_2$ ,  $TC_1$ , and  $TC_2$  from Table IV. We use the following technology nodes for this study: 7nm, 10nm and 14nm, and run *ChipletPart* on the four aforementioned testcases. Figure 11 presents the normalized chiplet costs (normalized to the cost of *manual* solutions) and the normalized runtime (represented as “Normalized Value” in Figure 11), normalized to a constant value of 10000 seconds.<sup>24</sup> In our experiments, we systematically vary each hyperparameter while keeping the others fixed at their default values. For each configuration, we measure the resulting chiplet cost and runtime across the testcases. Our observations from Figure 11 indicates that the default hyperparameter settings achieve a balanced trade-off between partitioning quality and runtime efficiency.

Figure 12 summarizes the sensitivity of *ChipletPart* to its hyperparameters. We measure sensitivity as the normalized variance in cost and runtime across the sweep range for each hyperparameter. Notably, crossover and mutation probability have the highest influence on cost, while population size and number of generations dominate runtime variation. Tournament size has relatively low sensitivity for both metrics. These results indicate that careful tuning of crossover and mutation parameters is essential for chiplet solution quality, while population size control primarily affects runtime overhead.

### C. Runtime remarks

*ChipletPart* is implemented entirely in C++, including a high-quality C++ translation of the Python-based cost model from [10]. Our optimized C++ translation achieves approximately a  $5\times$  speedup compared to the original Python version. Empirical results indicate that *ChipletPart*, when integrated with the translated C++ cost model, attains over a  $100\times$  speedup relative to an integration based on the Python cost model. Additionally, our open-sourced implementation is fully parallelized using OpenMP. These improvements make *ChipletPart* readily adaptable for any chiplet-based design flow.

We present a detailed runtime breakdown of *ChipletPart* in Table VII. Approximately 67% of the execution time is spent during floorplanning, while 28% is spent on chiplet

<sup>24</sup>10000 seconds is chosen for normalization to allow for comparison with about three hours of runtime.

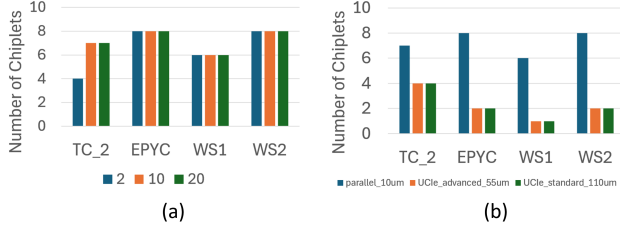


Fig. 13: (a) Reach limit vs. #chipllets. The partitioning solutions are generated with *ChiplletPart* using reach values of 2mm, 10mm and 20mm. (b) IO type vs. #chipllets.

cost evaluation. Further details on *ChiplletPart*’s runtime are provided in Table VI.

**Scalability.** For large designs such as WS<sub>4</sub>, our runtime remains under two hours. To improve scalability further, hierarchical decomposition techniques that exploit structural regularity in the netlist, along with aggressive solution pruning and potential usage of surrogate models for faster evaluation, can be employed.

## VII. ADDITIONAL CASE STUDIES

We investigate how different technology parameters affect *ChiplletPart*’s solutions. To accommodate an arbitrarily complex cost model, *ChiplletPart* employs a black-box partitioning method rather than a mathematical programming approach. This design choice enables a broader exploration of the parameter space compared to other partitioners. To illustrate these benefits, we present case studies that examine effects of altering cost model parameters.

**IO type and reach.** Chipllet systems often use reduced-size IO cells that trade driver strength and ESD protection for a smaller form factor. However, limited IO reach makes it challenging to generate feasible solutions. A 2mm reach may only allow direct connections between adjacent chipllets, while a larger reach (20mm) increases flexibility but also adds to system cost by increasing chipllet area. To explore this, we: (i) analyze the impact of IO reach on chipllet partitioning for a parallel IO testcase; and (ii) compare it with UCIE advanced and UCIE standard definitions [31], which have different cell sizes and reach. The parallel IO has 2mm reach, while the UCIE cases have 10mm reach.

Figure 13(a) shows that increasing reach enables a greater number of chipllets in the partitioning solution, while a short 2mm reach forces more blocks to remain together in fewer chipllets. This can be seen by looking at TC<sub>2</sub>. Figure 13(b) compares the same parallel IO testcase with UCIE interfaces, showing that UCIE’s large IO cells favor fewer chipllets, while the parallel interface with smaller IOs and bump pitches enables finer partitioning.

**Mixed cost/power objective function.** *ChiplletPart* can simultaneously optimize cost and power using a weighted sum of chipllet cost (Equation 1) and power as its objective

TABLE VIII: Effects of different cost and power coefficient combinations. Cost<sub>N</sub> and Power<sub>N</sub> refer to normalized cost and power, respectively.

Coefficients		WS <sub>1</sub>			TC <sub>1</sub>		
Cost	Power	C	Cost <sub>N</sub>	Power <sub>N</sub>	C	Cost <sub>N</sub>	Power <sub>N</sub>
1	0	6	<b>1.00</b>	<b>1.00</b>	6	<b>1.00</b>	<b>1.00</b>
0.75	0.25	6	1.02	0.97	4	1.03	0.97
0.5	0.5	4	1.06	0.95	2	1.04	0.95
0.25	0.75	4	1.07	0.93	2	1.07	0.93
0	1	2	1.10	0.92	1	1.08	0.91

function. Table VIII shows results for various cost and power coefficient combinations. For this experiment, we use the WS<sub>1</sub> and TC<sub>1</sub> testcases, with all chipllets implemented in 7nm technology. We see that increasing the power coefficient leads to fewer chipllets as large IO drivers for inter-chipllet connections have higher power.

## VIII. CONCLUSION

We have proposed *ChiplletPart*, a novel chipllet partitioning framework designed to tackle the challenges of partitioning large, 2.5D heterogeneously integrated systems into chipllets. *ChiplletPart* leverages an advanced cost model, is power-aware, and uses a genetic algorithm to simultaneously assign technologies to chipllets, all while consistently returning IO-feasible solutions that honor the driving reach of inter-chipllet IO drivers. Experimental results demonstrate that *ChiplletPart* outperforms classical netlist partitioners, *FloorPlet* [7], and human baselines. Additional studies illuminate dependencies of partitioning outcomes on the underlying packaging and IO technology.

While *ChiplletPart* is designed as a cost-driven partitioning framework, its modular, black-box optimization approach readily supports integration of more complex objective functions that consider power, performance and thermal factors. Extending the current objective function to include additional factors remains a direction for future work. Considering detailed IO planning is also another direction for future work. Detailed IO planning that supports pass-through connections, multiple IO types on a die, routing congestion, use of “gas station” buffers [56], buffer chipllets, or other similar architectural considerations will bring significantly increased problem complexity. We also aim to enhance *ChiplletPart* by identifying repeated structures in the netlist, a capability that could significantly improve scalability for larger problems. Finally, we are exploring the use of alternate optimizers, such as ILP, RL or BO. We also plan to integrate *ChiplletPart* with OpenROAD [57] to promote engagement in benchmarking and further development.

## REFERENCES

- [1] W. Gomes *et al.*, “Ponte vecchio: A multi-tile 3d stacked processor for exascale computing,” in *Proc. ISSCC*, 2022, pp. 42–44.

- [2] A. Sangiovanni-Vincentelli *et al.*, “Automated design of chiplets,” in *Proc. ISPD*, 2023, pp. 1–8.
- [3] A. Graening, S. Pal, and P. Gupta, “Chiplets: how small is too small?” in *Proc. DAC*, 2023, pp. 1–6.
- [4] G. Karypis *et al.*, “Multilevel hypergraph partitioning: applications in vlsi domain,” *IEEE Trans. on VLSI*, vol. 7, no. 1, pp. 69–79, 1999.
- [5] I. Bustany *et al.*, “Specpart: A supervised spectral framework for hypergraph partitioning solution improvement,” in *Proc. ICCAD*, 2022, pp. 1–9.
- [6] I. Bustany *et al.*, “An open-source constraints-driven general partitioning multi-tool for vlsi physical design,” in *Proc. ICCAD*, 2023, pp. 1–9.
- [7] S. Chen *et al.*, “Floorplet: performance-aware floorplan framework for chiplet integration,” *IEEE Trans. on CAD*, vol. 43, no. 6, pp. 1638–1649, 2023.
- [8] F. Li *et al.*, “Chipletizer: repartitioning socs for cost-effective chiplet integration,” in *Proc. ASP-DAC*, 2024, pp. 58–64.
- [9] A. Graening *et al.*, “Catch: a cost analysis tool for co-optimization of chiplet-based heterogeneous systems,” 2025. [Online]. Available: <https://arxiv.org/abs/2503.15753>
- [10] A. Graening, S. Pal, and P. Gupta, “Catch chiplets cost model.” <https://github.com/nanocad-lab/CATCH>, 2025.
- [11] “Chipletpart repository.” <https://github.com/ABKGroup/ChipletPart/blob/main/README.md>, 2025.
- [12] Y. Feng and K. Ma, “Chiplet actuary: a quantitative cost model and multi-chiplet architecture exploration,” in *Proc. DAC*, 2022, pp. 121–126.
- [13] Z. Zhuang *et al.*, “Multi-package co-design for chiplet integration,” in *Proc. ICCAD*, 2022, pp. 1–9.
- [14] A. Graening *et al.*, “Cost-performance co-optimization for the chiplet era,” in *2024 IEEE 26th Electronics Packaging Technology Conference (EPTC)*, 2024, pp. 40–45.
- [15] M. A. Kabir and Y. Peng, “Chiplet-package co-design for 2.5d systems using standard asic cad tools,” in *Proc. ASP-DAC*, 2020, pp. 351–356.
- [16] G. Karypis and V. Kumar, “Parallel multilevel k-way partitioning scheme for irregular graphs,” in *Proc. Conf. on SC*, 1996, pp. 35–35.
- [17] C. R-Vicharra, Y. Chen, and J. Hu, “Ppac driven multi-die and multi-technology floorplanning,” arXiv preprint 2502.10932, 2025.
- [18] Y.-K. Ho and Y.-W. Chang, “Multiple chip planning for chip-interposer codesign,” in *Proc. DAC*, 2013, pp. 1–6.
- [19] C.-C. Lee and Y.-W. Chang, “Floorplanning for embedded multi-die interconnect bridge packages,” in *Proc. ICCAD*, 2023, pp. 1–8.
- [20] H.-W. Chiou *et al.*, “Chiplet placement for 2.5d ic with sequence pair based tree and thermal consideration,” in *Proc. ASP-DAC*, 2023, pp. 7–12.
- [21] W.-H. Liu, M.-S. Chang, and T.-C. Wang, “Floorplanning and signal assignment for silicon interposer-based 3d ics,” in *Proc. DAC*, 2014, pp. 1–6.
- [22] D. Aldous and U. Vazirani, “Go with the winners algorithms,” in *Proc. FOCS*, 1994, pp. 492–501.
- [23] B. L. Miller, D. E. Goldberg *et al.*, “Genetic algorithms, tournament selection, and the effects of noise,” *Complex systems*, vol. 9, no. 3, pp. 193–212, 1995.
- [24] G. Syswerda, “Uniform crossover in genetic algorithms.” in *Proc. ICGA*, vol. 3, 1989, pp. 2–9.
- [25] K. Deb, “An introduction to genetic algorithms,” *Sadhana*, vol. 24, pp. 293–315, 1999.
- [26] A. Stillmaker and B. Baas, “Scaling equations for the accurate prediction of cmos device performance from 180nm to 7nm,” *Integration*, vol. 58, pp. 74–81, 2017.
- [27] K. Heyman, “Sram scaling issues, and what comes next,” Feb. 2024. [Online]. Available: <https://semiengineering.com/sram-scaling-issues-and-what-comes-next/>
- [28] M. LaPedus, “Big trouble at 3nm,” Jun. 2018. [Online]. Available: <https://semiengineering.com/big-trouble-at-3nm/>
- [29] D. Patel, “The dark side of the semiconductor design renaissance – fixed costs soaring due to photomask sets, verification, and validation,” Aug. 2023. [Online]. Available: <https://www.semianalysis.com/p/the-dark-side-of-the-semiconductor>
- [30] A. Shilov, “TSMC’s estimated wafer prices revealed: 300mm wafer at 5nm is nearly \$17,000,” Sep. 2020. [Online]. Available: <https://www.tomshardware.com/news/tsmcs-wafer-prices-revealed-300mm-wafer-at-5nm-is-nearly-dollar17000>
- [31] “UCIe specification 1.0.” [Online]. Available: <https://www.uciexpress.org/team-3>
- [32] S. Pal *et al.*, “Designing a 2048-chiplet, 14336-core waferscale processor,” in *Proc. DAC*, 2021, pp. 1183–1188.
- [33] S. Pal *et al.*, “I/o architecture, substrate design, and bonding process for a heterogeneous dielet-assembly based waferscale processor,” in *Proc. ECTC*, 2021, pp. 298–303.
- [34] C. Fiduccia and R. Mattheyses, “A linear-time heuristic for improving network partitions,” in *19th Design Automation Conference*, 1982, pp. 175–181.
- [35] K. Helsgaun, “An effective implementation of the lin-kernighan traveling salesman heuristic,” *European Journal of Operational Research*, vol. 126, no. 1, pp. 106–130, 2000.
- [36] U. Von Luxburg, “A tutorial on spectral clustering,” *Statistics and computing*, vol. 17, pp. 395–416, 2007.
- [37] A. Likas, N. Vlassis, and J. J. Verbeek, “The global k-means clustering algorithm,” *Pattern recognition*, vol. 36, no. 2, pp. 451–461, 2003.
- [38] B. Bahmani *et al.*, “Scalable k-means++,” *arXiv preprint arXiv:1203.6402*, 2012.
- [39] C. Zhang *et al.*, “Graph edge partitioning via neighborhood heuristic,” in *Proceedings of the 23rd ACM SIGKDD International Conference on Knowledge Discovery and Data Mining*, 2017, pp. 605–614.
- [40] “Metis repository.” <https://github.com/KarypisLab/METIS>, 2024.
- [41] H. Abdi, “Z-scores,” *Encyclopedia of measurement and statistics*, vol. 3, pp. 1055–1058, 2007.
- [42] “Kl refinement (klrefiner.cpp),” <https://github.com/ABKGroup/ChipletPart/blob/main/src/KLRefiner.cpp>, 2025.
- [43] “Reach violation calculation,” <https://github.com/ABKGroup/ChipletPart/blob/693f2fc09b0c85283e851ee783871080ed660afe/src/floorplan.cpp#L576>.
- [44] H. Murata *et al.*, “Vlsi module placement based on rectangle-packing by the sequence-pair,” *IEEE Trans. on CAD*, vol. 15, no. 12, pp. 1518–1524, 1996.
- [45] S. Kirkpatrick, C. D. Gelatt, and M. P. Vecchi, “Optimization by simulated annealing,” *Science*, vol. 220, no. 4598, pp. 671–680, 1983.
- [46] T.-C. Chen and Y.-W. Chang, “Modern floorplanning based on b\*-tree and fast simulated annealing,” *IEEE Trans. on CAD*, vol. 25, no. 4, pp. 637–650, 2006.
- [47] “Openmp library,” <https://www.openmp.org/>, 2021.
- [48] “Eigen v.3.4.0.” [https://eigen.tuxfamily.org/index.php?title=Main\\_Page](https://eigen.tuxfamily.org/index.php?title=Main_Page), 2021.
- [49] “Boost library v.1.87.0.” <https://www.boost.org/>, 2024.
- [50] B. Landman and R. Russo, “On a pin versus block relationship for partitions of logic graphs,” *IEEE Trans. on Computers*, vol. C-20, no. 12, pp. 1469–1479, 1971.
- [51] P. Singh and D. Landis, “Optimal chip sizing for multi-chip modules,” *IEEE Trans. on CPMT*, vol. 17, no. 3, pp. 369–375, 1994.
- [52] M. Cavalcante *et al.*, “Mempool: a shared-l1 memory many-core cluster with a low-latency interconnect,” in *Proc. DATE*, 2021, pp. 701–706.
- [53] M. Hempel and J. Redford, “Personal communication,” October 2024.
- [54] “AMD EPYC 7282.” [Online]. Available: <https://www.techpowerup.com/cpu-specs/epyc-7282.c2255>
- [55] “NVIDIA GA100.” [Online]. Available: <https://www.techpowerup.com/gpu-specs/nvidia-ga100.g931>
- [56] A. Coskun *et al.*, “Cross-layer co-optimization of network design and chiplet placement in 2.5-d systems,” *IEEE Trans on CAD*, vol. 39, no. 12, pp. 5183–5196, 2020.
- [57] “The openroad project,” <https://github.com/The-OpenROAD-Project/OpenROAD>.